Cell, Vol. 100, 435–446, February 18, 2000, Copyright ©2000 by Cell Press

Ras1 Promotes Cellular Growth in the *Drosophila* Wing

David A. Prober and Bruce A. Edgar*
Molecular and Cellular Biology Program
and Program in Developmental Biology
Fred Hutchinson Cancer Research Center
Seattle, Washington 98109
University of Washington
Seattle, Washington 98195

Summary

The Ras GTPase links extracellular mitogens to intracellular mechanisms that control cell proliferation. To understand how Ras regulates proliferation in vivo, we activated or inactivated Ras in cell clones in the developing *Drosophila* wing. Cells lacking Ras were smaller, had reduced growth rates, accumulated in G1, and underwent apoptosis due to cell competition. Conversely, activation of Ras increased cell size and growth rates and promoted G1/S transitions. Ras upregulated the growth driver dMyc, and both Ras and dMyc increased levels of cyclin E posttranscriptionally. We propose that Ras primarily promotes growth and that growth is coupled to G1/S progression via cyclin E. Interestingly, upregulation of growth by Ras did not deregulate G2/M progression or a developmentally regulated cell cycle exit.

Introduction

Mitotically proliferating cells generally coordinate rates of cell cycle progression with rates of cellular growth (i.e., mass accumulation). Elegant studies in yeast have demonstrated that rates of cellular growth dictate rates of cell cycle progression (Johnston et al., 1977). This relationship was recently extended to proliferating imaginal cells in *Drosophila melanogaster*, where it was found that reducing rates of cellular growth coordinately reduces rates of cell cycle progression, whereas altering rates of cell cycle progression has little effect on growth (Weigmann et al., 1997; Neufeld et al., 1998). However, the mechanisms that coordinate growth with the cell cycle in multicellular organisms remain poorly understood.

The Ras protooncogene is an important regulator of cell proliferation and thus could play a role in coordinating growth with the cell cycle. Ras acts as a molecular switch by adopting either an active conformation upon binding GTP or an inactive conformation while bound to GDP. This property is used by a variety of signal transduction pathways to transmit signals from cell surface receptors, usually receptor tyrosine kinases, to signaling molecules within a cell, notably Raf and the MAP kinase (MAPK) pathway (reviewed by Rommel and Hafen, 1998).

Ras is involved in coordinating growth with the cell cycle in *Saccharomyces cerevisiae*, where activation of the Ras/cAMP pathway by improved nutrient conditions increases cell size (reviewed by Thevelein and de Winde, 1999). This reflects an increase in the rate of cellular growth relative to the rate of cell cycle progression. Conversely, inhibition of the Ras pathway results in a G1 cell cycle arrest similar to that observed upon nutrient depletion (Kataoka et al., 1985). Ras has also been implicated in regulating cell proliferation in mammals, most strikingly by the observation that mutationally activated forms of Ras are present in a wide spectrum of tumors (reviewed by Barbacid, 1987). Furthermore, activation of Ras in transformed human and mouse cell lines can shorten G1 phases and accelerate cell proliferation (Liu et al., 1995; Winston et al., 1996; Fan and Bertino, 1997). In contrast, inhibition of Ras causes a G1 arrest in NIH 3T3 cells (Mulcahy et al., 1985) and mouse embryo fibroblasts (Leone et al., 1997; Mittnacht et al., 1997; Peeper et al., 1997), which in the latter case was shown to require the Retinoblastoma (Rb) tumor suppressor. These studies have led to a general model wherein activation of Ras by growth factors leads to hyperphosphorylation of Rb, releasing the transcription factor E2F to transcribe genes required for S phase progression. While this model may explain how Ras regulates cell cycle progression, its role in regulating cellular growth, which is required to maintain a consistent cell size in proliferating cells, remains unclear.

We have addressed the role of Ras in regulating cellular growth and proliferation in the developing *Drosophila* wing. *Drosophila* has three Ras homologs, but only Dras1 has substantial homology to mammalian *ras* (75% identity; Neuman-Silberberg et al., 1984) and participates in the MAPK signaling pathway (Fortini et al., 1992; Lu et al., 1993; Asha et al., 1999). In *Drosophila*, Dras1 (hereafter referred to as Ras) has been implicated in regulating many processes, including cell proliferation (Karim and Rubin, 1998), differentiation (Fortini et al., 1992), patterning (Schnorr and Berg, 1996), apoptosis (Bergmann et al., 1998; Kurada and White, 1998), and cell migration (Lee et al., 1996).

Considerable evidence indicates that Ras is required for growth and/or cell survival during wing development. The wing develops as a monolayer of epithelial cells, the imaginal disc, that originates from an embryonic primordium of about 50 cells. During the 4 days of larval development, the disc grows, and its cells proliferate exponentially to reach a final size of 50,000 cells at the onset of differentiation. These cells roughly double their mass during every 8–12 hr cell cycle. Loss-of-function mutations in several members of the Ras/MAPK pathway result in larvae with small or missing imaginal discs (Nishida et al., 1988; Clifford and Schupbach, 1989; Biggs et al., 1994; Simcox et al., 1996). Furthermore, wing cell clones lacking components of the Ras/MAPK pathway fail to survive to adulthood (Diaz-Benjumea and Hafen, 1994). Vein, a secreted ligand homologous to mammalian neuregulins (Schnepp et al., 1996), and its receptor, the *Drosophila* EGF receptor (Livneh et al., 1985), activate the Ras pathway and are required for

*To whom correspondence should be addressed (e-mail: bedgar@fred.fhcrc.org).

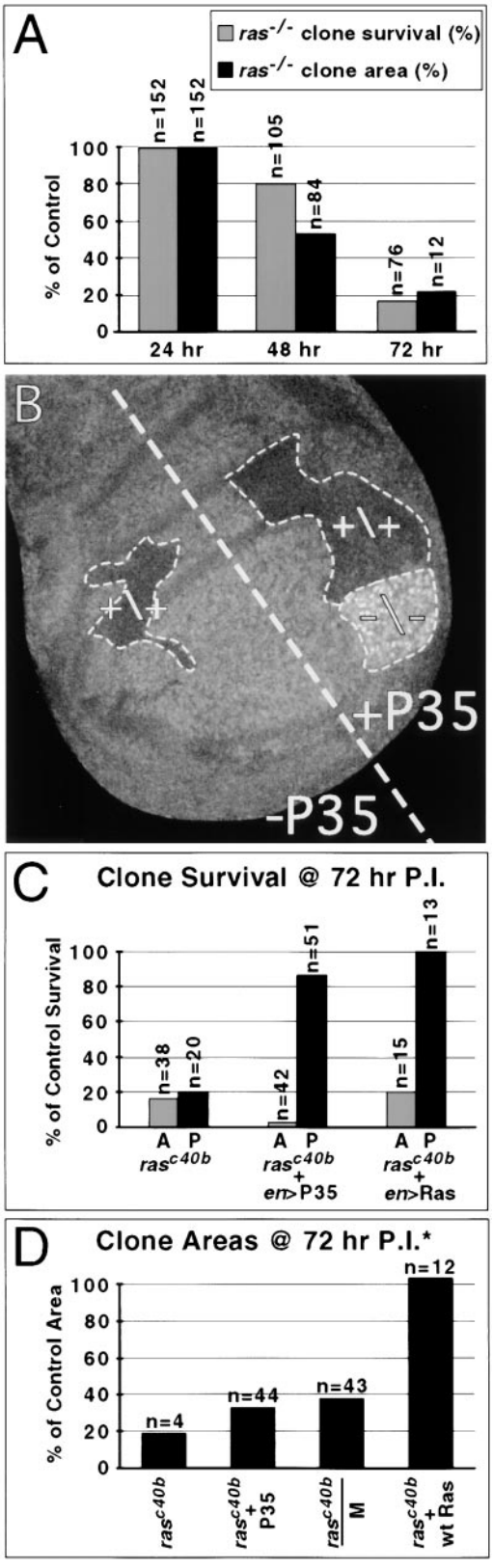

Figure 1. Loss of Ras Slows Cell Growth and Leads to Cell Death

(A) The frequency and size of *ras*$^{c40b/c40b}$ (*ras*$^{-/-}$) clones decline over time. Clones were induced at 48, 72, or 96 hr after egg deposition (AED) and analyzed at 120 hr AED. Gray bars represent the percentage of *ras*$^{+/+}$ clones (twinspots) that are paired with *ras*$^{-/-}$ clones. Black bars represent the median areas of *ras*$^{-/-}$ clones as a percentage of the median areas of their *ras*$^{+/+}$ sister clones. n = number of *ras*$^{+/+}$ clones counted (gray bars) or number of *ras*$^{-/-}$ and *ras*$^{+/+}$ pairs analyzed (black bars).

(B) Rescue of *ras*$^{-/-}$ clone viability by ectopic expression of P35 in the posterior compartment. *ras*$^{-/-}$ cells are marked with two copies of π-myc while ras$^{+/+}$ cells lack π-myc staining. Dashed line indicates approximate position of the anterior-posterior border. Posterior is to the right.

(C) *ras*$^{-/-}$ clone survival defect is rescued by P35. Clones were induced at 48 hr AED and analyzed 72 hr postinduction (P. I.) at 120 hr AED. The percentage of *ras*$^{+/+}$ clones that are paired with *ras*$^{-/-}$ clones in the anterior (A) and posterior (P) compartments are shown. Note that P35 and Ras are only expressed in posterior compartments, so anterior compartments serve as internal controls. n = number of *ras*$^{+/+}$ clones counted. Genotypes: left, HS-FLP^{122}; +/En-Gal4; FRT (82B) *ras*^{c40b} π-myc/FRT (82B), middle, HS-FLP^{122}; UAS-P35/En-Gal4; FRT (82B) *ras*^{c40b} π-myc/FRT (82B), right, HS-FLP^{122}; UAS-Ras/En-Gal4; FRT (82B) *ras*^{c40b} π-myc/FRT (82B).

(D) *ras*$^{-/-}$ clone size defect is partially rescued by P35 and by reduced cell competition. Median areas of *ras*$^{-/-}$ clones as percentages of median areas of their *ras*$^{+/+}$ sister clones in the posterior compartment from (C) are shown. *Due to the developmental delay of *M(3)95A* heterozygotes, clones in these lines were induced at 72 hr AED and analyzed at 144 (*M*$^{+/+}$) or 168 (*ras*$^{-/-}$*M*$^{+/+}$) hr AED, which approximately corresponded to normal developmental times of 48 and 120 hr AED. n = number of *ras*$^{-/-}$ and *ras*$^{+/+}$ pairs analyzed. Genotypes: as in (C), except HS-FLP^{122};+; FRT (82B) π-myc/FRT (82B) *M(3)95A* and HS-FLP^{122};+; FRT (82B) *ras*^{c40b} π-myc/FRT (82B) *M(3)95A*.

growth of the wing (Clifford and Schupbach, 1989; Simcox, 1997).

It has also been shown that expression of an activated form of Ras at the anterior-posterior boundary of the wing disc can induce cell proliferation and widespread cell death (Karim and Rubin, 1998). However, interpreting these results is problematic because the region of the disc where Ras was activated serves as a major pattern organizing center. Hence, the observed effects may have been non–cell autonomous consequences of altered cell fates therein. To avoid the potential complications of region-specific modulation of Ras activity, we have activated or inactivated Ras in marked cell clones generated at random locations throughout the wing disc. We have analyzed the cell-autonomous effects of Ras activity on cellular growth, cell cycle progression, and cell cycle rates. Our findings suggest a model for how Ras coordinates cellular growth and cell cycle progression in the wing.

Results

Cells Lacking Ras Have Poor Viability

Previous studies showed that cells lacking *ras* are eventually eliminated from the developing wing (Diaz-Benjumea and Hafen, 1994). To determine whether this is due to defects in cell proliferation or cell survival, we tested the proliferative capability of *ras*$^{-/-}$ cells using the *ras*^{c40b} allele, in which the entire *ras* open reading frame is deleted (Schnorr and Berg, 1996). Using FLP/FRT-mediated mitotic recombination (Xu and Rubin, 1993) in larvae heterozygous for *ras*^{c40b}, we generated two clonal populations from single cells, one homozygous for *ras*^{c40b} (*ras*$^{-/-}$) and the other homozygous for wild-type

ras (*ras*$^{+/+}$). We analyzed clones 24, 48, and 72 hr after induction and observed a gradual decline in both the number of *ras*$^{-/-}$ clones present and in the size (in area) of surviving *ras*$^{-/-}$ clones compared to their *ras*$^{+/+}$ sister clones ("twinspots") (Figure 1A). Nuclear staining of *ras*$^{-/-}$ clones revealed many pyknotic nuclei, a morphological characteristic of cell death. These results suggest that cells lacking *ras* have poor viability. However, even 72 hr following induction, relatively large *ras*$^{-/-}$ clones containing 40–80 cells were observed, albeit at a low frequency. Thus, *ras* is not absolutely required for cell proliferation and survival. Expression of wild-type *ras* in posterior wing compartments using the Engrailed-Gal4 driver completely rescued both the survival (Figure 1C) and size (Figure 1D) of *ras*$^{-/-}$ clones, indicating that loss of *ras* was indeed responsible for these phenotypes.

To further test the requirement of *ras* for cell survival, *ras*^{c40b} clones were generated in discs in which the apoptosis inhibitor P35 (Hay et al., 1994) was expressed in posterior wing compartments (Figure 1B). P35 increased the survival of *ras*$^{-/-}$ clones from 2% to 86% (Figure 1C), indicating that the loss of *ras*$^{-/-}$ clones results from apoptosis. P35 also increased the size of *ras*$^{-/-}$ clones compared to their *ras*$^{+/+}$ sisters, although there was still a large size difference between them (Figure 1D). Since blocking apoptosis only partially restored the size of *ras*$^{-/-}$ clones, we conclude that cells lacking *ras* have reduced rates of both cell proliferation and survival.

Ras Is Required to Promote Growth and Inhibit Apoptosis Resulting from Cell Competition

Having established that Ras is important for long-term cell survival, we examined the basis of this requirement. Ras might specifically inhibit molecules in the wing that promote cell death, as it does *hid* in the *Drosophila* eye (Bergmann et al., 1998; Kurada and White, 1998). Alternatively, Ras might promote growth, and the death of *ras*$^{-/-}$ cells may result from cell competition, a phenomenon in which slowly growing cells are eliminated by faster growing neighbors (Morata and Ripoll, 1975). If *ras*$^{-/-}$ cells die due to slowed growth, they should survive better and produce larger clones if given a growth advantage. However, if Ras inhibits a death-promoting signal, a growth advantage should not alter clone survival or size. To distinguish between these possibilities, we gave *ras*$^{-/-}$ cells a growth advantage using the *Minute(3)95A* mutation. *M(3)95A* is a dominant, loss-of-function mutation in the ribosomal protein rpS3 (Andersson et al., 1994), which is cell lethal when homozygous and slows cell growth when heterozygous, presumably by limiting protein synthesis. Thus, *M*$^{+/+}$ cells have a growth advantage over *M*$^{+/-}$ cells. Clones of *ras*$^{-/-}$*M*$^{+/+}$ cells were generated in discs that were heterozygous for both mutations, thus reducing competitive pressure on the *ras*$^{-/-}$ cells. Since no sister clones were generated in this experiment due to the inviability of *M*$^{-/-}$ cells, we compared *ras*$^{-/-}$*M*$^{+/+}$ clones to control *M*$^{+/+}$ clones in separate *M*$^{+/-}$ discs. In parallel experiments, 20 discs containing *ras*$^{-/-}$*M*$^{+/+}$ clones and 22 discs containing control *M*$^{+/+}$ clones were required to obtain 43 clones each. Thus, *ras*$^{-/-}$*M*$^{+/+}$ clones were recovered at a frequency similar to that of *M*$^{+/+}$ control clones, a much improved clone survival rate compared with *ras*$^{-/-}$ clones in a wild-type background (Figure 1C). The areas of *ras*$^{-/-}$*M*$^{+/+}$ clones were 38% that of *M*$^{+/+}$ controls (Figure 1D). In comparison, the areas of *ras*$^{-/-}$ clones in a wild-type background were 19% as large as their *ras*$^{+/+}$ sister clones (Figure 1D). Since *ras*$^{-/-}$ clones in a *Minute* background had increased survival rates and were larger than *ras*$^{-/-}$ clones in a wild-type background, we infer that *ras* promotes growth, leading to cell survival by reducing cell competition.

Table 1. Cell Size Measurements in Different Cell Cycle Phases

Genotype	FSC G1 + S + G2	FSC G1	FSC S + G2
Figure 2 Data			
Control	0.99	0.99	1.00
Ras^{N17}	0.97	0.97	0.97
Ras^{V12}	1.13	1.12	1.09
Figure 4 Data			
Control	0.95	0.93	0.98
Ras^{V12}	1.17	1.15	1.16
Stg	0.90	0.91	1.00
Ras^{V12} + Stg	0.94	0.97	0.98
RBF	1.07	1.07	1.09
Ras^{V12} + RBF	1.26	1.24	1.26

Forward scatter (FSC) ratios for cells in all phases of the cell cycle, cells in G1, and cells in S and G2 are shown. Values represent ratios of GFP$^+$ mean FSC (experimental) to GFP$^-$ mean FSC (internal control). FSC ratios are virtually identical in all cell cycle phases for cells of a particular genotype.

Inhibition of Ras Reduces Cell and Clone Growth

As a second approach to inhibit Ras function, we generated clones coexpressing green fluorescent protein (GFP) and a dominant-negative form of Ras (Ras^{N17}) using the flip-out technique (Struhl and Basler, 1993). Ras^{N17} is preferentially maintained in its GDP-bound inactive conformation and is thought to sequester the guanine nucleotide exchange factor Sos, thereby preventing activation of endogenous Ras (Feig and Cooper, 1988). The flip-out technique allows generation of permanent, heritable expression of UAS-regulated transgenes in random clones of cells at precise time points during development. Discs containing GFP-expressing clones were analyzed by fluorescent activated cell sorting (FACS). This allowed comparison of forward scatter (FSC) values, which provide a relative measure of cell size, of cells coexpressing GFP + Ras^{N17} to nonexpressing control cells. Expression of Ras^{N17} caused a small but reproducible decrease in mean FSC values in all phases of the cell cycle (Figure 2A; Table 1), indicating that Ras^{N17} reduces cell size. While this suggests that Ras^{N17} reduces cellular growth, we wished to assess this more directly. Since the area of a clone reflects the growth of all cells within it during the time between clone induction and analysis, we measured the areas of individual Ras^{N17}-expressing clones to determine the effect on clonal growth rates. Since Ras^{N17} causes cell death (see below), we compared clones coexpressing Ras^{N17} + P35 with clones expressing P35 alone. Forty-four hours after induction, clones coexpressing Ras^{N17} + P35 were 23% smaller than clones expressing P35

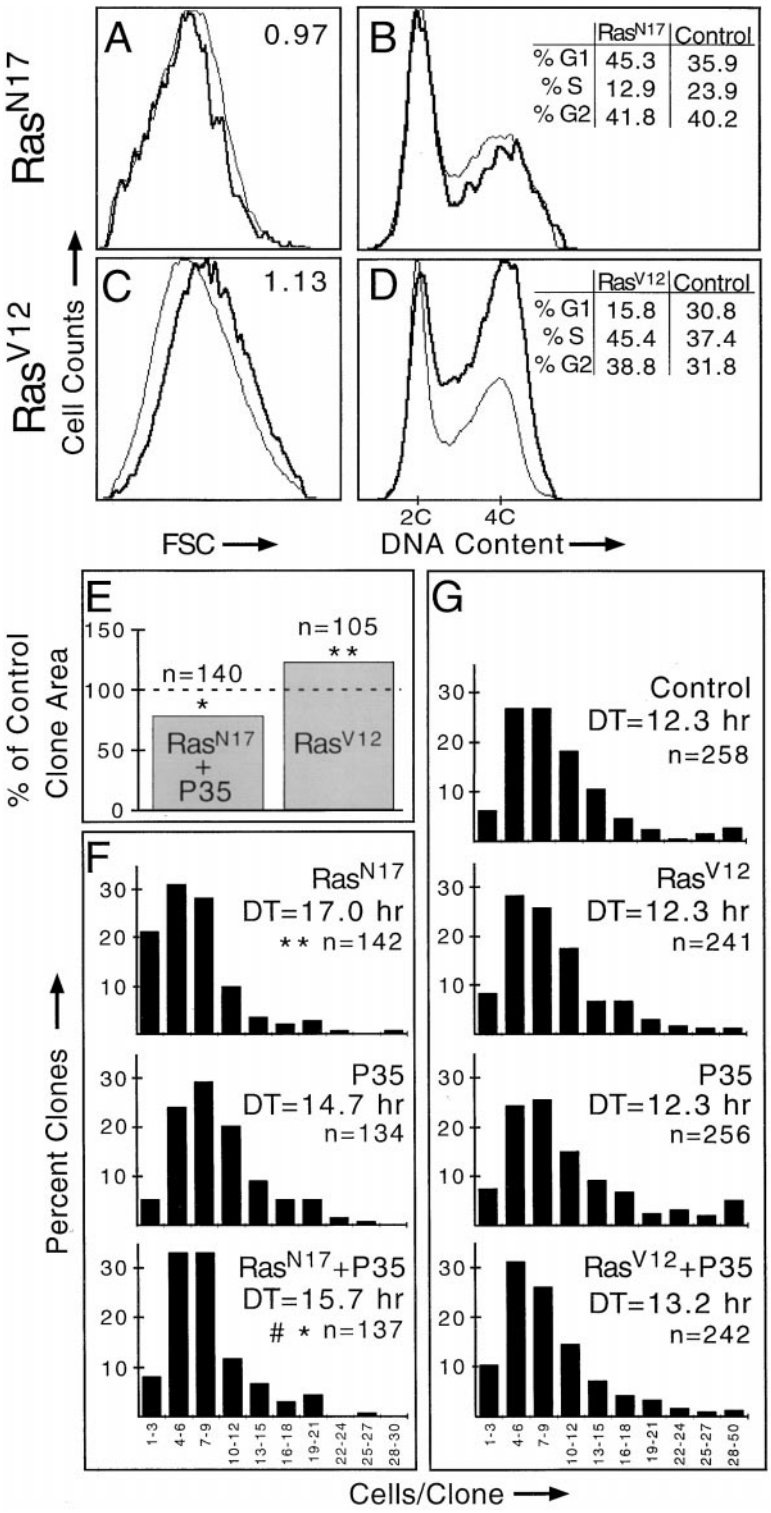

Figure 2. Effects of Ras Activity on Cell Size, Cell Cycle Progression, Clone Size, and Cell Division Rate

(A–D) Ras^{N17} and Ras^{V12} have opposite effects on cell size and cell cycle phasing. Clones expressing Ras^{N17} (A and B) or Ras^{V12} (C and D) were induced at 48 hr AED and analyzed by FACS at 96 hr AED. Dark trace represents GFP^+ (experimental), and light trace represents GFP^- (wild-type) cells. Numbers in (A) and (C) represent the ratio of GFP^+ mean FSC to GFP^- mean FSC for data shown. Control samples expressing GFP alone analyzed in parallel had an FSC ratio of 0.99. In (B) and (D), the percentage of cells in each phase of the cell cycle for GFP^+ and GFP^- cells are shown.

(E) Ras^{N17} and Ras^{V12} have opposite effects on clone size. The median area of clones expressing Ras^{N17} + P35 or Ras^{V12} divided by the median area of clones expressing P35 or GFP alone, respectively, is shown. Clones expressing Ras^{N17} were induced at 72 hr AED and analyzed at 116 hr AED. Ras^{V12}-expressing clones were induced at 58 hr AED and analyzed at 94 hr AED. The number of clones scored (n) is indicated. Clone areas significantly different from their controls are marked with asterisks (*, $p < 0.05$; **, $p < 0.01$).

(F) Ras^{N17} slows the cell cycle and induces apoptosis. Clones were induced at 72 hr AED and analyzed at 116 hr AED. The number of cells per clone as a percentage of the total number of clones analyzed for each genotype is plotted. Median cell doubling times (DT) and the number of clones scored (n) are indicated in each panel. Doubling times significantly different from P35 are marked with asterisks (*, $p < 0.05$; **, $p < 0.01$). # indicates $p < 0.05$ compared with Ras^{N17} alone.

(G) Ras^{V12} does not affect the cell doubling time. Clones were induced at 81 hr AED and analyzed at 118 hr AED. Ras^{V12} doubling times were also the same as control at 48–73, 58–94, and 77–118 hr AED. None of the doubling times are significantly ($p < 0.05$) different from control.

alone (Figure 2E). We conclude that reduction of Ras activity decreases cellular and clonal growth rates, resulting in decreased cell and clone sizes.

Activation of Ras Increases Cell and Clone Growth

FACS analysis was also performed on discs containing flip-out clones expressing Ras^{V12}, which is preferentially maintained in the GTP-bound conformation and thus is constitutively active (Barbacid, 1987). Ras^{V12} expression increased mean FSC values in all phases of the cell cycle (Figure 2C; Table 1). Microscopic observation confirmed that cells expressing Ras^{V12} were considerably larger than wild-type cells (Figures 3A–3D) and demonstrated that Ras^{V12} expression did not disrupt the monolayer

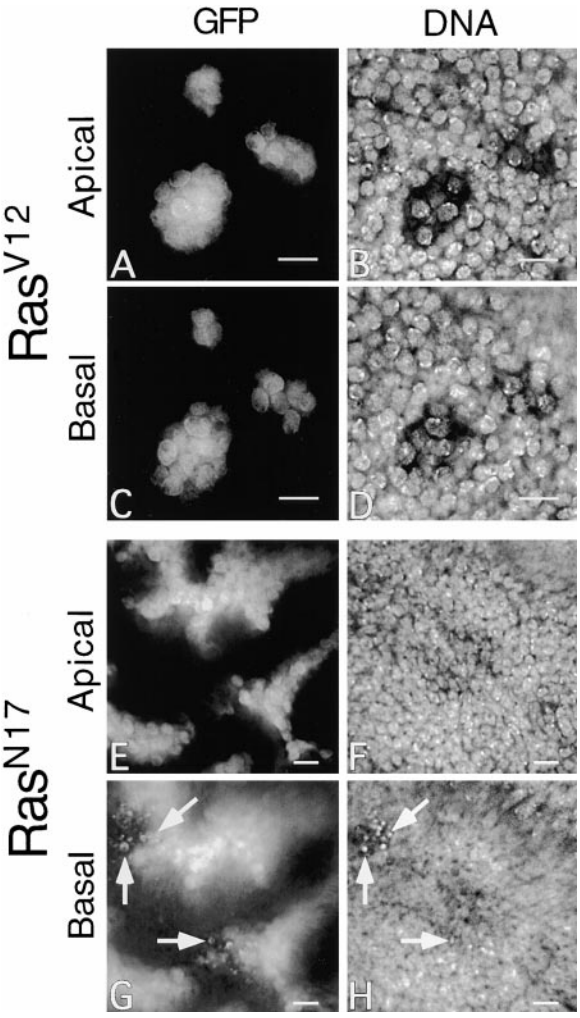

Figure 3. Morphology of Clones Expressing Activated or Dominant-Negative Ras

(A–D) Cells expressing Ras^{V12} (GFP^{+} cells in [A] and [C]) are larger than neighboring cells, as indicated by reduced nuclear density ([B] and [D]), and mix poorly with neighboring cells.

(E–H) Cells expressing Ras^{N17} (GFP^{+} cells in [E] and [G]) mix well with neighboring cells. Basal section shows GFP^{+} pyknotic nuclei (arrows in [G] and [H]), indicating cell autonomous cell death. Scale bars = 10 μm.

structure of the tissue (data not shown). Furthermore, the areas of Ras^{V12}-expressing clones were 21% larger than those of control clones expressing GFP alone when measured 36 hr after induction (Figure 2E). Thus, Ras^{V12} accelerates rates of cellular and clonal growth, resulting in increased cell and clone sizes. Interestingly, Ras^{V12}-expressing clones were round with smooth borders (Figures 3A and 3C), suggesting that they have altered affinities and thus resist mixing with nonexpressing cells.

Effect of Ras Activity on Cell Doubling Time

We also measured cell division rates by counting the number of cells in clones expressing Ras^{N17} or Ras^{V12}. Clones expressing Ras^{N17} had fewer cells than control clones expressing GFP alone and thus contained cells with longer apparent doubling times (Figure 2F). As with *ras*$^{-/-}$ clones, Ras^{N17} expression caused cell death (Figures 3G and 3H, arrows). Coexpressing P35 with Ras^{N17} completely suppressed cell death (data not shown) and increased the number of cells per clone (Figure 2F). However, blocking apoptosis only partially rescued the cell doubling time defect. Thus, Ras^{N17}-expressing cells divide more slowly than controls. In contrast, expression of Ras^{V12} had no effect on cell doubling times (Figure 2G). To test whether shorter doubling times were being masked by apoptosis, we coexpressed P35 with Ras^{V12}. This did not shorten apparent cell doubling times (Figure 2G). Consistent with this result, we did not observe elevated levels of cell death in Ras^{V12}-expressing clones (data not shown). Thus, Ras^{V12} has no effect on cell division rates in the developing wing.

Ras Promotes the G1/S Transition

As cell growth and the cell cycle appear to be linked during wing development (Neufeld et al., 1998), we tested whether altering Ras activity affected cell cycle phasing. Expression of Ras^{N17} caused an increase in the proportion of cells in G1 and a decrease in the proportion of cells in S phase (Figure 2B). Conversely, expression of Ras^{V12} reduced the G1 cell population and increased the proportions of cells in S and G2 (Figure 2D). This suggests that Ras promotes G1/S transitions in wing imaginal cells, as it does in mammalian cell culture (Downward, 1997) and budding yeast (Hall et al., 1998).

Since the doubling time of cells expressing Ras^{V12} is normal, they may compensate for a truncated G1 by lengthening S and G2. Alternatively, the primary effect of Ras^{V12} may be to elongate S and G2, with cells compensating by accelerating progression through G1. To distinguish these possibilities, we coexpressed Ras^{V12} and String (Stg), the Cdc25-type phosphatase that is rate limiting for G2/M progression in *Drosophila* (Neufeld et al., 1998). If the primary effect of Ras^{V12} is to shorten G1, shortening G2 as well by coexpressing Stg should accelerate cell proliferation. However, if the primary effect of Ras^{V12} is to lengthen S and G2, bypassing this effect by coexpressing Stg should not accelerate cell proliferation. As previously shown (Neufeld et al., 1998), expression of Stg greatly reduced the G2 cell population (Figure 4A, right), but cells compensated by lengthening G1 and only had a slightly shorter doubling time (Figure 4A, left). When Ras^{V12} + Stg were coexpressed, the doubling time was even shorter (Figure 4A, left). We conclude that the primary effect of Ras^{V12} expression on the cell cycle is to shorten G1 and that extension of S and G2 is a secondary effect.

While ectopic Ras^{V12} made cells larger and overexpressed Stg made cells slightly smaller, coexpression of both genes resulted in cells of normal size (Figure 4A, middle; Table 1). In contrast, large G1 and small G2 cell populations were observed upon expression of Stg alone or when Ras^{V12} + Stg were coexpressed (Figure 4A, right). Thus, the extended G2 period induced by Ras^{V12} can be overcome by ectopic Stg expression. At the same time, the areas of clones either coexpressing Ras^{V12} + Stg or expressing Ras^{V12} alone were significantly larger than those of controls (Figure 4B). Thus, the ability of Ras^{V12} to increase the rate of clonal growth is independent of both the size and cell cycle phasing of cells in the clone.

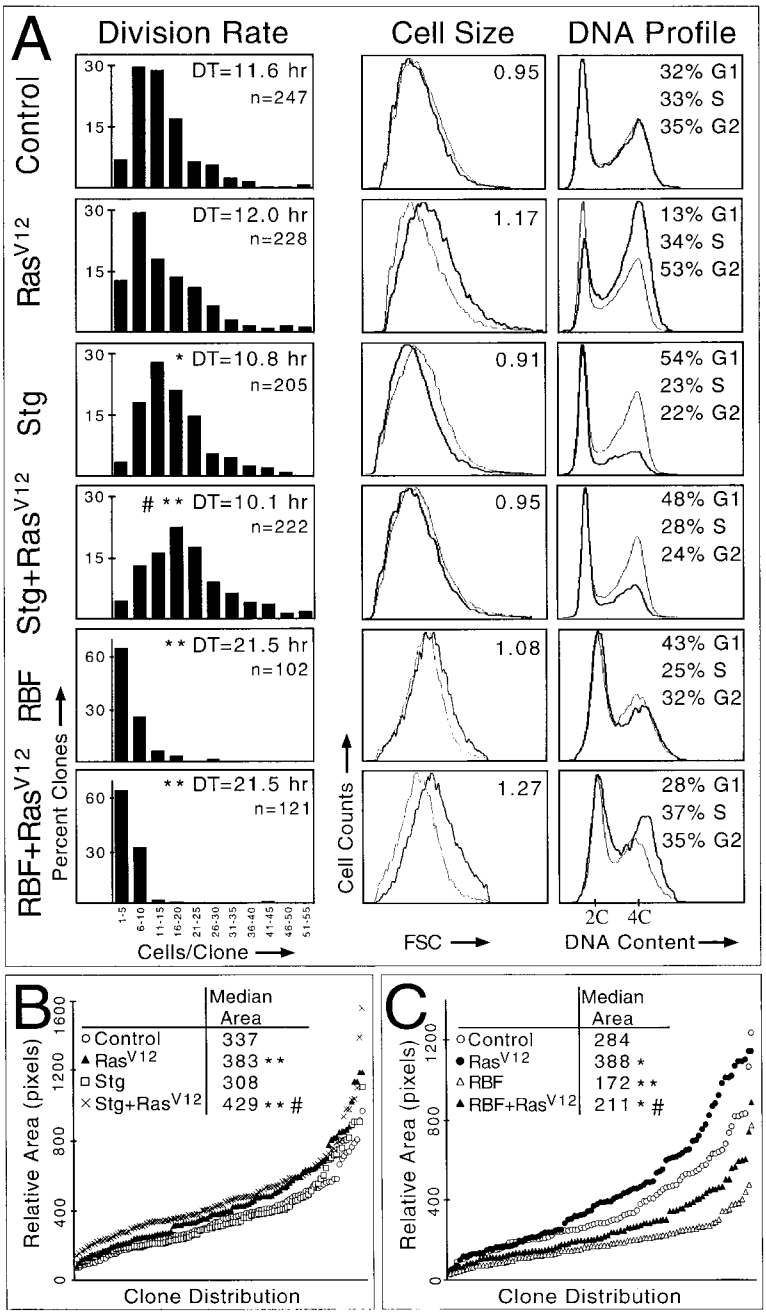

Figure 4. Interaction of Ras^{V12} with Cell Cycle Regulators

(A) Left column, cell doubling time. Clones were induced at 74 hr AED and analyzed at 117 hr AED. While expressing Ras^{V12} alone has no effect and expressing Stg alone causes a slightly shorter cell doubling time, coexpressing Ras^{V12} + Stg results in an even shorter cell doubling time. Overexpressing RBF results in a longer cell doubling time, and coexpressing Ras^{V12} + RBF does not antagonize this effect. Cell doubling times significantly different from control are marked with asterisks (*, $p < 0.05$; **, $p < 0.01$). # indicates $p < 0.01$ compared with Stg alone. Clones expressing RBF ± Ras^{V12} were analyzed on a separate day, with similar doubling times for control and Ras^{V12} to those shown here.

Middle column, cell size. Clones were induced at 67 hr AED and analyzed at 115 hr AED. Forward scatter (FSC) data indicates that expressing Ras^{V12} increases cell size, expressing Stg decreases cell size, and coexpressing Ras^{V12} + Stg results in a wild-type cell size. Coexpressing Ras^{V12} + RBF has an additive effect on cell size compared to expression of either Ras^{V12} or RBF alone. Dark trace represents GFP$^+$ (experimental) and light trace represents GFP$^-$ (wild-type) cells. Numbers represent ratio of GFP$^+$ mean FSC to GFP$^-$ mean FSC for data shown. Right column, cell cycle. Clones for control, Ras^{V12}, and Stg ± Ras^{V12} were induced at 45 hr AED and analyzed at 95 hr AED. Clones for RBF ± Ras^{V12} were induced at 72 hr AED and analyzed at 120 hr AED. The effect of Stg on cell cycle phasing is dominant to Ras^{V12}, while the effect of Ras^{V12} is dominant to RBF. Dark trace represents GFP$^+$ (experimental), and light trace represents GFP$^-$ (wild-type) cells. Percentage of GFP$^+$ cells in each phase of the cell cycle is indicated.

(B) Ras^{V12} increases clonal growth independent of String. Clone area measurements for Ras^{V12} + Stg samples whose doubling times are shown in (A). Clones either coexpressing Ras^{V12} + Stg or expressing Ras^{V12} alone are larger than clones expressing either Stg or GFP alone. Each data point represents the relative area of a single clone. One hundred and eleven clones were scored for each genotype. ** indicates $p < 0.01$ compared with control. # indicates $p < 0.01$ compared with Stg alone. Since clones coexpressing Ras^{V12} + Stg are larger than control but contain normal sized cells, they must contain more cells, which thus have shorter doubling times, than controls.

(C) Ras^{V12} increases clonal growth independent of RBF. Clone area measurements for Ras^{V12} + RBF samples whose doubling times are shown in (A). Clones coexpressing Ras^{V12} + RBF are larger than clones expressing RBF alone by an amount similar to that of clones expressing Ras^{V12} compared with GFP alone. Each data point represents the relative area of a single clone.

Ninety-three clones were scored for each genotype. Mean clone areas significantly different from control are marked with asterisks (*, $p < 0.05$; **, $p < 0.01$). # indicates $p < 0.01$ compared with RBF alone.

Ras Does Not Inhibit the Rb Homolog RBF

To further explore the interaction of Ras with the cell cycle machinery, we tested whether Ras might drive G1/S transitions by inhibiting the *Drosophila* Rb homolog, RBF. Clonal overexpression of RBF slows all phases of the cell cycle, resulting in large cells with extended doubling times (Figure 4A, left and middle; Neufeld et al., 1998). If Ras inhibits RBF, then coexpression of Ras^{V12} + RBF should suppress these effects. However, coexpression of Ras^{V12} + RBF did not suppress the inhibitory effect of RBF on cell cycle rates (Figure 4A, left). Furthermore, Ras^{V12} + RBF coexpression had an additive effect on cell size (Figure 4A, middle; Table 1). Consistent with these results, clones coexpressing Ras^{V12} + RBF were larger than those expressing RBF alone (Figure 4C), even though they had the same number of cells. In fact, the

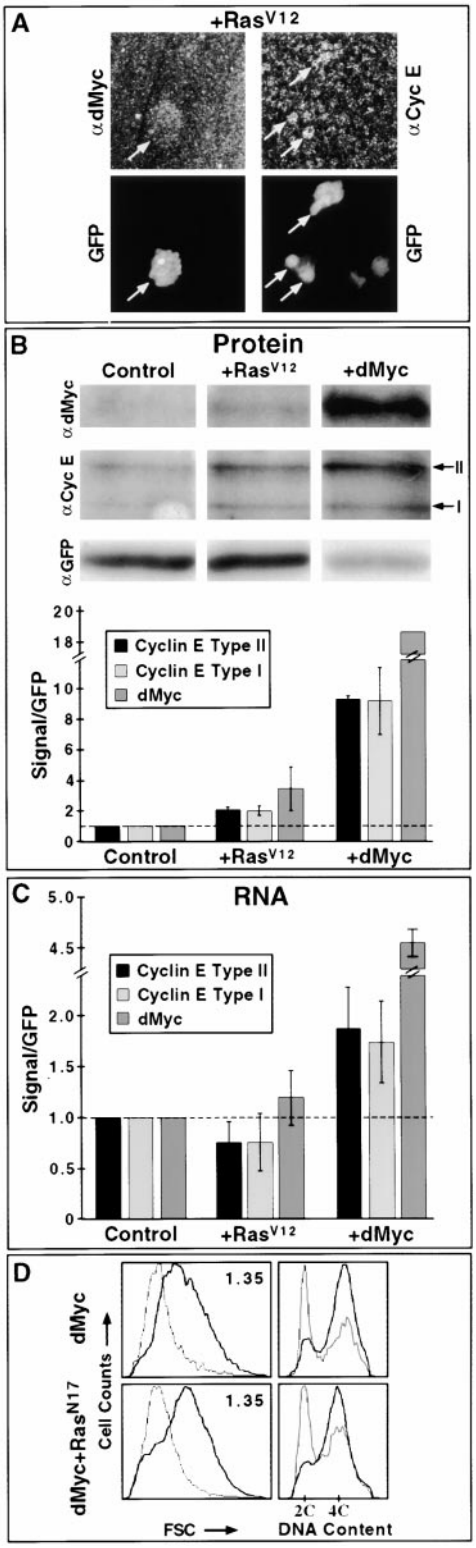

Figure 5. Ras^{V12} Upregulates dMyc and Cyclin E Posttranscriptionally

(A) Left column, cells expressing Ras^{V12} (GFP, arrow) have elevated levels of dMyc protein (αdMyc, arrow). Magnification = 400×. Right column, cells expressing Ras^{V12} (GFP, arrows) have elevated levels of cyclin E protein (αCycE, arrows). Magnification = 630×. Increased dMyc or cyclin E staining was not observed in control clones expressing GFP alone.

increase in clone area was similar to that of Ras^{V12}-expressing clones compared to controls. Cells coexpressing Ras^{V12} + RBF also had shorter G1 phases than cells expressing RBF alone (6.0 hr versus 9.2 hr; Figure 4A). These results indicate that overexpressed Ras^{V12} does not inhibit overexpressed RBF and suggest that the ability of Ras^{V12} to upregulate growth and drive G1/S transitions is independent of RBF's inhibitory effect on cell cycle progression.

Ras Upregulates dMyc

dMyc, the *Drosophila* homolog of the Myc transcription factor, has similar effects on growth and the cell cycle to Ras. Cells lacking dMyc are small, grow slowly, and are subject to cell competition, while cells overexpressing dMyc have accelerated growth and a truncated G1 (Johnston et al., 1999). dMyc is a stronger growth driver than Ras^{V12}, suggesting that Ras may be acting via dMyc. To determine whether Ras upregulates dMyc, we stained Ras^{V12}-expressing clones with a dMyc-specific antibody. We observed slightly elevated levels of dMyc protein in Ras^{V12}-expressing cells (Figure 5A). To confirm this result, we performed Western blots on discs in which most cells coexpressed Ras^{V12} + GFP. These discs contained 3.4-fold more dMyc protein than controls expressing GFP alone (Figure 5B). To determine whether this effect was transcriptional, we performed quantitative reverse transcription-polymerase chain reaction (RT-PCR) on these discs. There was no significant increase in *dmyc* transcript levels (Figure 5C). Thus, activation of Ras elevates dMyc protein levels posttranscriptionally.

We next analyzed the functional relationship between Ras and dMyc. To determine whether dMyc can rescue the growth defects resulting from inhibition of Ras, we generated flip-out clones coexpressing dMyc and Ras^{N17}. FACS analysis revealed cell size and cell cycle profiles similar to those of cells expressing dMyc alone (Figure 5D). Furthermore, dMyc expression partially rescued the elongated cell doubling time of 17.2 hr for Ras^{N17} to 15.5 hr for Ras^{N17} + dMyc ($p = 0.015$; dMyc alone = 12.6 hr). These results suggest that the effects of Ras on cellular growth and the cell cycle are at least partially mediated via dMyc.

(B) Western blot. Each lane contains approximately 20 wing discs expressing GFP alone (control), Ras^{V12} + GFP, or dMyc + GFP. Arrows indicate the cyclin E type I and II isoforms. Measured intensities of cyclin E– and dMyc-specific bands relative to GFP are shown below. Data represent mean values ± standard deviation from at least two experiments. Due to developmental delay, discs expressing dMyc were slightly smaller than controls and thus had less total protein/lane.

(C) RT-PCR. RNA from discs expressing GFP alone (control), Ras^{V12} + GFP, or dMyc + GFP was isolated and subjected to quantitative fluorescent RT-PCR. Relative levels of *cyclin E* and *dmyc* transcripts were quantified and normalized to *gfp*. Data represent mean values ± standard deviation from samples analyzed in triplicate.

(D) dMyc is dominant to Ras^{N17}. Clones coexpressing dMyc + Ras^{N17} were induced at 72 hr AED and analyzed at 120 hr AED. Dark trace represents GFP$^+$ (experimental) and light trace represents GFP$^-$ (wild-type) cells. Numbers represent the ratio of GFP$^+$ mean FSC to GFP$^-$ mean FSC.

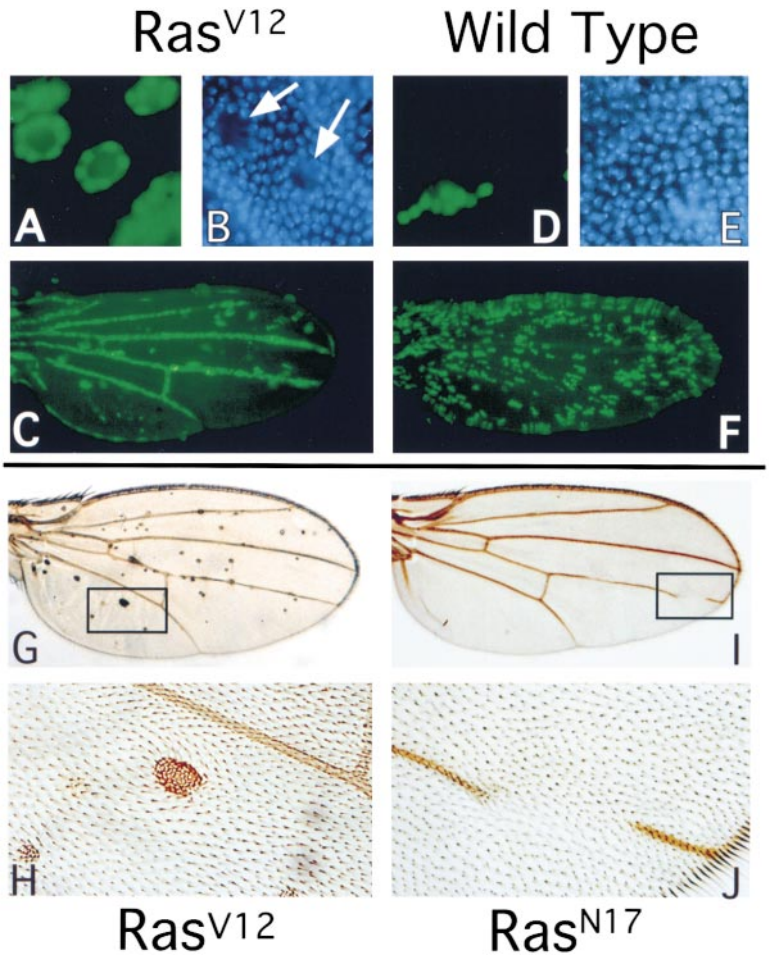

Figure 6. Effects of Ectopic Ras Expression in Pupal and Adult Wings

Clones expressing Ras^{V12} (A–C) or GFP alone (D–F) were induced at 96 hr AED and analyzed at 24 (A, B, D, and E) or 36 (C and F) hr APF. Many intervein Ras^{V12}-expressing clones form rosette-like structures, with nuclei in the center of clones dropping basally or disappearing completely (arrows in [B]). By 36 hr APF, clones expressing Ras^{V12} become concentrated in regions of developing vein tissue (C), while control clones expressing GFP alone remain evenly distributed throughout the wing (F). Clones expressing Ras^{V12} induced at 72 hr AED produce ectopic vein-like cuticle in adult wings (G and H), while Ras^{N17} expression deletes vein tissue (I and J). Boxed areas in (G) and (I) are shown at higher magnification in (H) and (J), respectively.

Ras^{V12} and dMyc Upregulate Cyclin E

We next sought to analyze the effect of Ras and dMyc on G1/S progression. Cyclin E is rate limiting for G1/S progression in wing discs (Neufeld et al., 1998). Both the type I and II isoforms of *cyclin E* contain open reading frames in their 5′ untranslated regions (Richardson et al., 1993), which could potentially render translation of cyclin E sensitive to growth rates (see the Discussion). We therefore tested whether increasing the rate of cellular growth by expressing Ras^{V12} or dMyc increases levels of cyclin E protein. Cells expressing Ras^{V12} had slightly elevated levels of cyclin E protein when stained with a cyclin E–specific antibody (Figure 5A). In addition, Western blots revealed a 2-fold increase of both the type I and II isoforms of cyclin E in response to Ras^{V12} expression (Figure 5B). Consistent with the stronger effects of dMyc on growth and G1/S progression, expression of dMyc caused a 9-fold increase of both cyclin E isoforms (Figure 5B). These increases were posttranscriptional, since little or no increase in *cyclin E* transcript levels was observed by RT-PCR (Figure 5C). Thus, posttranscriptional control of cyclin E appears to couple cellular growth rates to G1/S progression.

Cells Expressing Ras^{V12} Arrest and Differentiate on Schedule

In many systems, cells expressing activated Ras are resistant to signals that promote quiescence or differentiation, and Ras activation is often associated with cell transformation (Barbacid, 1987). We therefore asked whether cells expressing Ras^{V12} in the wing were capable of arresting and differentiating in a normal fashion at the end of larval development. We induced clones during larval development and analyzed them in pupal and adult wings. Approximately 24 hr after pupal formation (APF), both Ras^{V12} and control clones were evenly distributed throughout the developing vein and intervein regions of the wing (data not shown). However, the nuclei of cells in the center of some intervein Ras^{V12} clones dropped basally or disappeared completely (Figures 6A and 6B), suggesting that they were being eliminated. Later in development (36 hr APF), most Ras^{V12}-expressing clones became concentrated in developing vein regions (Figure 6C), while control clones remained evenly distributed throughout the wing (Figure 6F). Staining with an antibody specific to activated MAP kinase indicated that endogenous Ras is strongly activated in the future vein regions of late larval and early pupal wing discs and is only weakly active in intervein regions (data not shown; Gabay et al., 1997; Guichard et al., 1999). Thus, our observations suggest that cells possessing inappropriate levels of Ras activity are eliminated from intervein regions at the onset of differentiation.

When larger Ras^{V12}-expressing clones were generated, many intervein clones survived and formed ectopic vein-like cuticle in adult wings (Figures 6G and 6H). Conversely, clones expressing Ras^{N17} failed to make veins in adult wings (Figures 6I and 6J). Therefore, Ras is

necessary and sufficient to form vein-like tissue, consistent with reports implicating the Ras pathway in vein development (Clifford and Schupbach, 1989; Sturtevant et al., 1993; Brunner et al., 1994; Diaz-Benjumea and Hafen, 1994; Sturtevant and Bier, 1995; Karim and Rubin, 1998; Guichard et al., 1999). Importantly, these results demonstrate that cells expressing activated Ras do not proliferate indefinitely and are able to differentiate at the appropriate time in development, provided they reside in the proper spatial context.

Discussion

Ras Promotes Growth

Cellular growth, defined as accumulation of mass, accompanies most cell divisions and allows cells to maintain a consistent cell size. Despite our knowledge of how cell division is regulated, we know little about how cells monitor their size to coordinate growth with the cell cycle. Here, we demonstrate that Ras, a major effector of extracellular signals, functions in vivo in the *Drosophila* wing to regulate cellular growth. When Ras activity was reduced, using either a null allele or by expressing a dominant-negative allele of Ras, growth slowed, cell size decreased, and cell death due to cell competition increased. Conversely, activation of Ras increased growth rates and cell size. As the Ras/cAMP pathway regulates cellular growth in response to nutrient levels in budding yeast (Thevelein and de Winde, 1999), our results indicate that growth regulation by Ras is conserved in both single and multicelled organisms. However, we unexpectedly found that activation of Ras was not sufficient to accelerate cell division. This contrasts with Ras's ability to increase cell cycle rates in isolated cell culture systems (Liu et al., 1995; Fan and Bertino, 1997). Our data indicate that this difference is due to Ras-independent control of G2/M progression in vivo. In addition, our work implies that, contrary to expectation, increased growth is not sufficient to accelerate cell proliferation.

Ras Affects the Cell Cycle by Regulating Growth

We found that in addition to promoting growth, Ras activity also controls the length of G1. This has also been observed in mammalian cells, and it has been suggested that Ras promotes cell proliferation by acting on components of the cell cycle machinery that regulate G1/S progression (reviewed by Downward, 1997). Although *Drosophila* Ras might promote G1/S progression and cellular growth independently, our observations suggest that in the developing wing, its primary effect is to promote growth, and its cell cycle effects are secondary. Hence, we propose the model shown in Figure 7. This model is supported by our findings that Ras continued to promote growth when coexpressed with Stg, which reversed the cell cycle effects of Ras, and when coexpressed with RBF, which had a dominant effect to Ras in slowing the cell cycle (Figure 4). This contrasts with the proposal that the role of Ras in cell cycle progression is to inhibit Rb by directing its phosphorylation (Leone et al., 1997; Mittnacht et al., 1997; Peeper et al., 1997).

Other proteins that promote growth, such as the *Drosophila* homologs of Myc (dMyc; Johnston et al., 1999)

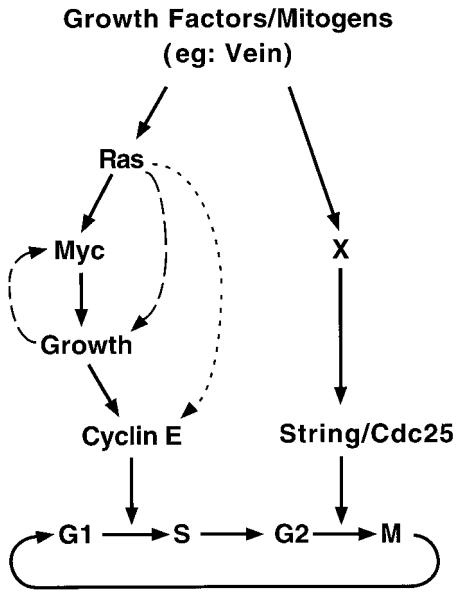

Figure 7. Model for Cell Cycle Regulation in *Drosophila* Wing Disc Cells

We propose that there is parallel and independent control of G1/S and G2/M transitions in *Drosophila* wing disc cells. Cellular growth due to Ras or dMyc drives G1/S transitions by promoting translation of cyclin E. Ras may also drive growth via proteins other than dMyc; this could feed back to upregulate translation of *dmyc* mRNA (dashed arrows). Alternatively, Ras may regulate cellular growth and the G1/S cell cycle machinery in parallel (dotted arrow). Stg/Cdc25, which is regulated primarily at the transcriptional level, drives G2/M transitions. Signaling molecules capable of regulating coordinated growth and patterning such as Vein may regulate G1/S transitions via Ras, dMyc, or other growth-promoting proteins and regulate G2/M transitions via transcription factors (X) that modulate transcription of Stg/Cdc25.

and Phosphoinositide 3-Kinase (dPI3K; Weinkove et al., 1999), have effects on cell cycle progression similar to Ras. Upregulating these proteins in the developing wing truncates G1, elongates G2, and increases growth rates, while downregulating them causes opposing effects. Furthermore, the resulting growth rates are inversely proportional to the length of G1. Given these similarities, we propose that cellular growth is rate limiting for G1/S progression in wing imaginal cells.

Cyclin E Couples Growth to the Cell Cycle

How might cellular growth drive G1/S transitions? Coupling of cellular growth to G1/S progression might be explained by a mechanism in which unstable, translationally regulated proteins are rate limiting for G1/S transitions. Cyclin E, a short-lived protein, is rate limiting for G1/S progression in wing discs (Neufeld et al. 1998). We found that both Ras^{V12} and dMyc posttranscriptionally increased levels of cyclin E (Figures 5A–5C). As with the yeast G1 cyclin Cln3, the 5′ untranslated region of *Drosophila cyclin E* contains several open reading frames (uORFs; Richardson et al., 1993). Polymenis and Schmidt (1997) proposed that the Cln3 uORF reduces initiation of translation at the downstream Cln3 translation start site. As a result, more ribosomes are needed to achieve efficient translation of Cln3. Since the abundance of ribosomes correlates with growth rate (Warner,

1999), the uORF renders translation of Cln3 sensitive to the rate of cellular growth. Our data suggest that a similar mechanism may regulate production of cyclin E in the developing wing. Cyclin E would thus act as a "growth sensor" to couple growth rates to G1/S progression. This hypothesis could be tested by mutating the cyclin E uORFs and assaying how cyclin E protein levels and G1/S progression respond to ectopic Ras or dMyc.

Ras May Promote Growth via dMyc

Our data suggest that the effects of Ras on cellular growth and the cell cycle are at least partially mediated by dMyc. Mammalian Myc transcription factors activate expression of many genes involved in cellular growth and metabolism (Dang, 1999), and *Drosophila* dMyc is a potent growth driver in vivo (Johnston et al., 1999). Upregulation of dMyc by Ras appears to be posttranscriptional. Ras might act by inhibiting degradation of dMyc protein, as has been demonstrated in mammalian cell culture (Sears et al., 1999). Alternatively, Ras might stimulate growth via other proteins, such as components of the dPI3K/dAkt/dS6 Kinase pathway, which promote cellular growth in *Drosophila* (Montagne et al., 1999; Weinkove et al., 1999; Verdu et al., 1999). Increased growth due to these proteins could then feed back to promote translation of extant *dmyc* mRNA. However, dMyc and dPI3K cannot be mediating all of Ras's effects, since unlike Ras they do not affect cell fate or cell adhesion (Johnston et al., 1999; Weinkove et al., 1999). These additional functions of Ras, along with the ability to increase Myc protein levels, likely contribute to the strong synergistic action of Ras and Myc in oncogenesis (Land et al., 1983; Sinn et al., 1987).

G1/S, But Not G2/M, Is Regulated by Growth

Ras^{V12} accelerated G1/S transitions but failed to accelerate rates of cell division (Figure 2). This is similar to our findings with overexpressed dMyc (Johnston et al., 1999). However, coexpressing either Ras^{V12} or dMyc with String (Stg), the G2/M rate limitor, did accelerate cell division. This suggests that regulation of Stg is independent of both Ras and dMyc. We therefore propose that there is parallel and independent control of G1/S and G2/M transitions during wing development (Figure 7). Signaling molecules capable of regulating coordinated growth and patterning, such as Vein, Decapentaplegic, and Wingless might control G1/S transitions by regulating growth via Ras, dMyc, or other growth-promoting proteins. These signaling molecules might also, unlike Ras and dMyc, control G2/M transitions by modulating transcription of *stg*. Analysis of more than 40 kb of the *stg* promoter has revealed an extensive array of regulatory modules that respond to different patterning signals and thus integrate complex patterning information (Lehman et al., 1999). A model in which cyclin E acts as a growth sensor and Stg acts as a "pattern sensor" is attractive, as it allows coordination of independent growth and patterning signals by the cell cycle machinery.

This model is supported not only by experiments but also by characteristics of normal development. Early in wing development (36–96 hr AED), rapid growth and cell proliferation take place, and as the disc prepares to differentiate into an adult wing (96–148 hr AED), growth and proliferation slow (Garcia-Bellido and Merriam, 1971). During the rapid growth phase, cells express *stg* RNA uniformly and at high levels and have a very short G2 (L. A. Johnston, personal communication; Neufeld et al., 1998). This suggests that cell cycle length is primarily regulated at G1/S and that growth may thus be rate limiting for cell proliferation at this stage. As growth slows near the end of wing development, disc cells express *stg* periodically (Milan et al., 1996) and in patterns (Johnston and Edgar, 1998) and acquire a much longer G2 (Fain and Stevens, 1982; Graves and Schubiger, 1982; Neufeld et al., 1998). Thus, at a time when many detailed patterning decisions are being made, cell cycle length may become primarily regulated by Stg at G2/M.

Ras, Growth, and Cancer

Studies of the role of Ras in cancer have focused on its role in driving quiescent cells into the cell cycle, its ability to promote G1/S transitions in cycling cells, and its effects on cell adhesion and the cytoskeleton. In contrast, little is known regarding its role in promoting cellular growth. We have found that *Drosophila* Ras, like vertebrate Ras, promotes G1/S transitions and alters the adhesive properties and identities of cells. Significantly, we have also shown that Ras promotes growth and that its effects on the cell cycle are secondary. This suggests that activation of Ras, as well as other oncogenes such as Myc, may promote cancer by driving cellular growth. In light of this, it is interesting to note that *Drosophila* disc cells increase their mass 6-fold prior to exiting a developmentally regulated G1 cell cycle arrest early in larval development (Madhavan and Schneiderman, 1977). The increase in cellular mass suggests that cellular growth may be promoting exit from this arrest. By analogy, the ability of Ras to promote exit from quiescence in cancer may also be a consequence of growth promotion. Consistent with this idea, cellular hypertrophy is commonly observed during neoplastic progression in mice (Iritani and Eisenman, 1999) and humans, suggesting that our findings are relevant to mammalian pathology.

Experimental Procedures

Fly Stocks and Transgenes

UAS-Ras^{N17} (II), Lee et al., 1996; UAS-Ras^{V12} (III), Karim and Rubin, 1998; UAS-Ras^{WT} (II), Karim and Rubin, 1998; UAS-P35 (II), Hay et al., 1994; UAS-String16 (II), Neufeld et al., 1998; UAS-RBF (III), N. Dyson; UAS-dMyc (III), Johnston et al., 1999; Actin 5c>CD2>Gal4, UAS-GFP_{NLS} S65T (III), Pignoni and Zipursky, 1997, and Neufeld et al., 1998; En-Gal4 (II), A. Brand; w; FRT (82B) ras^{c40b}/TM6B, Schnorr and Berg, 1996; w; FRT (82B) M(3)95A/TM6B, Andersson et al., 1994; and w; FRT (82B) π-myc.

ras^{c40b} Clonal Analysis

Clones were generated using the FLP/FRT method (Xu and Rubin, 1993). Fifty staged larvae from 2 hr egg collections were transferred upon hatching to vials containing yeast paste and raised at 25°C. Larvae were heat shocked for 45 min at 37°C at 48, 72, or 96 hr after egg deposition (AED), dissected at wandering (120 hr AED), and fixed in 4% paraformaldehyde/PBS. The π-myc clonal marker was detected as described (Neufeld et al., 1998). Discs were mounted in Fluoroguard (BioRad) and imaged on a Leica TCSSP confocal microscope. Clone areas were measured using the histogram function of Adobe Photoshop.

Flow Cytometry

Larvae raised as above were heat shocked for 1 hr at 37°C at various times during larval development, resulting in wing discs with approximately 50% of their cells GFP^+. FACS analysis was performed as described (Neufeld et al., 1998). Each experiment was performed at least twice.

Proliferation and Growth Rate Analysis

Clones expressing Gal4 were induced using the flip-out technique (Struhl and Basler, 1993; Pignoni and Zipursky, 1997; Neufeld et al., 1998) in HS-FLP^{122}; Act>CD2>Gal4, UAS-GFP_{NLS} S65T (± additional UAS transgenes) animals. Larvae raised as above were heat shocked at various times during development for 20–30 min at 37°C, producing 5–10 clones per disc, and were fixed and mounted as above. The number of GFP^+ cells per clone was counted on a Leitz DMRD microscope. Cell doubling times were derived using the formula (log 2/log N)hr, where N = median number of cells/clone and hr = time between heat shock and disc fixation. Clone areas were measured as above. *p* values were calculated using a two-tailed student's t-test. Each experiment was performed at least twice.

Histology

Hoechst 33258 (Acros) was used to stain nuclei. Cell death was visualized with Acridine Orange as described (Neufeld et al., 1998) or by observing pyknotic nuclear staining in the basal plane of the disc epithelium. Cyclin E (8B10) and dMyc (P4C4 B10) monoclonal antibodies were used and detected with a Cy3 anti-mouse secondary antibody (Jackson ImmunoResearch). High magnification fluorescent images were collected on a Deltavision S/A30 microscope.

Western Blots and RT-PCR

Larvae raised as above were heat shocked for 2.5 hr at 37°C at 72 hr AED and dissected at 120 hr AED. FACS analysis indicated that ~90% of the cells in these discs were GFP^+. Approximately 100 wing discs were removed and washed in PBS. For Western blots, discs were suspended in 10 μl SDS sample buffer and boiled. Following brief centrifugation, the supernatant was diluted to 1 disc/μl in SDS sample buffer and analyzed by SDS-polyacrylamide gel electrophoresis. Monoclonal antibodies were used to detect cyclin E (8B10) and dMyc (P2A7-A9), and a rabbit polyclonal antibody was used to detect GFP (Clontech). Primary antibodies were detected using HRP-conjugated secondary antibodies (Amersham) and visualized using the ECL system (Amersham). Multiple exposures of films were scanned, and protein quantitation was performed using ImageQuant (Molecular Dynamics). For RT-PCR, discs were suspended in Trizol Reagent (Gibco BRL), and RNA was isolated as instructed by the manufacturer. RT-PCR was performed using the TaqMan Gold RT-PCR Kit and the ABI Prism 7700 Sequence Detection System (PE Applied Biosystems) according to the manufacturer's instructions, using FAM-TAMRA fluorogenic probes (MWG Biotech). Relative transcript levels were determined using the relative standard curve and delta-delta Ct methods.

Acknowledgments

We thank Celeste Berg, Peter Gallant, Felix Karim, and Denise Montell for fly stocks; Robert Eisenman, Peter Gallant, and Helena Richardson for antibodies; Aida de la Cruz, Mary Kay Dolejsi (grant #5P30CA15704–26), Adrian Quintanilla, and the Fred Hutchinson Cancer Research Center Flow Cytometry and Image Analysis facilities for technical assistance; and Jon Cooper, Tom Neufeld, and members of the Edgar lab for helpful advice, discussions, and comments on the manuscript. D. A. P. is a National Science Foundation predoctoral fellow, and B. A. E. is a Rita Allen Scholar. This work supported by the National Institutes of Health (GM51186).

Received August 4, 1999; revised January 11, 2000.

References

Andersson, S., Saeboe-Larssen, S., Lambertsson, A., Merriam, J., and Jacobs-Lorena, M. (1994). A *Drosophila* third chromosome Minute locus encodes a ribosomal protein. Genetics *137*, 513–520.

Asha, H., de Ruiter, N.D., Wang, M.G., and Hariharan, I.K. (1999). The Rap1 GTPase functions as a regulator of morphogenesis in vivo. EMBO J. *18*, 605–615.

Barbacid, M. (1987). Ras genes. Annu. Rev. Biochem. *56*, 779–827.

Bergmann, A., Agapite, J., McCall, K., and Steller, H. (1998). The *Drosophila* gene *hid* is a direct molecular target of Ras-dependent survival signaling. Cell *95*, 331–341.

Biggs, W.H., Zavitz, K.H., Dickson, B., van der Straten, A., Brunner, D., Hafen, E., and Zipursky, S.L. (1994). The *Drosophila rolled* locus encodes a MAP kinase required in the sevenless signal transduction pathway. EMBO J. *13*, 1628–1635.

Brunner, D., Oellers, N., Szabad, J., Biggs, W.H., Zipursky, S.L., and Hafen, E. (1994). A gain-of-function mutation in *Drosophila* MAP Kinase activates multiple receptor tyrosine kinase signaling pathways. Cell *76*, 875–888.

Clifford, R.J., and Schupbach, T. (1989). Coordinately and differentially mutable activities of *torpedo*, the *Drosophila melanogaster* homolog of the vertebrate EGF receptor gene. Genetics *123*, 771–787.

Dang, C.V. (1999). c-Myc target genes involved in cell growth, apoptosis, and metabolism. Mol. Cell Biol. *19*, 1–11.

Diaz-Benjumea, F.J., and Hafen, E. (1994). The sevenless signaling cassette mediates *Drosophila* EGF receptor function during epidermal development. Development *120*, 569–578.

Downward, J. (1997). Cell cycle: routine role for Ras. Curr. Biol. *7*, R258-R260.

Fain, M.J., and Stevens, B. (1982). Alterations in the cell cycle of *Drosophila* imaginal disc cells precede metamorphosis. Dev. Biol. *92*, 247–258.

Fan, J., and Bertino, J.R. (1997). K-*ras* modulates the cell cycle via both positive and negative regulatory pathways. Oncogene *14*, 2595–2607.

Feig, L.A., and Cooper, G.M. (1988). Inhibition of NIH 3T3 cell proliferation by a mutant *ras* protein with preferential affinity for GDP. Mol. Cell. Biol. *8*, 3235–3243.

Fortini, M.E., Simon, M.A., and Rubin, G.M. (1992). Signaling by the *sevenless* protein tyrosine kinase is mimicked by Ras1 activation. Nature *355*, 559–561.

Gabay, L., Seger, R., and Shilo, B.Z. (1997). In situ activation pattern of *Drosophila* EGF receptor pathway during development. Science *277*, 1103–1106.

Garcia-Bellido, A., and Merriam, J.R. (1971). Parameters of the wing imaginal disc development in *Drosophila melanogaster*. Dev. Biol. *26*, 61–87.

Graves, B.J., and Schubiger, G. (1982). Cell cycle changes during growth and differentiation of imaginal leg discs in Drosophila melanogaster. Dev. Biol. *93*, 104–110.

Guichard, A., Biehs, B., Sturtevant, M.A., Wickline, L., Chacko, J., Howard, K., and Bier, E. (1999). *rhomboid* and *Star* interact synergistically to promote EGFR/MAPK signaling during *Drosophila* wing vein development. Development *126*, 2663–2676.

Hall, D.D., Markwardt, D.D., Parvitz, F., and Heideman, W. (1998). Regulation of the Cln3-Cdc28 kinase by cAMP in *Saccharomyces cerevisiae*. EMBO J. *17*, 4370–4378.

Hay, B.A., Wolff, T., and Rubin, G.M. (1994). Expression of baculovirus P35 prevents cell death in *Drosophila*. Development *120*, 2121–2129.

Iritani, B.M., and Eisenman, R.N. (1999). c-Myc enhances protein synthesis and cell size during B lymphocyte development. Proc. Natl. Acad. Sci. USA *96*, 13180–13185.

Johnston, L.A., and Edgar, B.A. (1998). Wingless and Notch regulate cell-cycle arrest in the developing *Drosophila* wing. Nature *394*, 82–84.

Johnston, G.C., Pringle, J.R., and Hartwell, L.H. (1977). Coordination of growth with cell division in the yeast *Saccharomyces cerevisiae*. Exp. Cell Res. *105*, 79–98.

Johnston, L.A., Prober, D.A., Edgar, B.A., Eisenman, R.N., and Gallant, P. (1999). *Drosophila myc* regulates cellular growth during development. Cell *98*, 779–790.

Karim, F.D., and Rubin, G.M. (1998). Ectopic expression of activated Ras1 induces hyperplastic growth and increased cell death in *Drosophila* imaginal tissues. Development *125*, 1–9.

Kataoka, T., Powers, S., Cameron, S., Fasano, O., Goldfarb, M., Broach, J., and Wigler, M. (1985). Functional homology of mammalian and yeast *ras* genes. Cell *40*, 19–26.

Kurada, P., and White, K. (1998). Ras promotes cell survival in *Drosophila* by downregulating *hid* expression. Cell *95*, 319–329.

Land, H., Parada, L.F., and Weinberg, R.A. (1983). Tumorigenic conversion of primary embryo fibroblasts requires at least two cooperating oncogenes. Nature *304*, 596–602.

Lee, T., Feig, L., and Montell, D.J. (1996). Two distinct roles for Ras in a developmentally regulated cell migration. Development *122*, 409–418.

Lehman, D.A., Patterson, B., Johnston, L.A., Balzer, T., Britton, J.S., Saint, R., and Edgar, B.A. (1999). *Cis*-regulatory elements of the mitotic regulator, *string*/*Cdc25*. Development *126*, 1793–1803.

Leone, G., DeGregori, J., Sears, R., Jakoi, L., and Nevins, J.R. (1997). Myc and Ras collaborate in inducing accumulation of active cyclin E/Cdk2 and E2F. Nature *387*, 422–426.

Liu, J.J., Chao, J.R., Jiang, M.C., Ng, S.Y., Yen, J.J.Y., and Yang-Yen, H.F. (1995). Ras transformation results in an elevated level of Cyclin D1 and acceleration of G1 progression in NIH 3T3 cells. Mol. Cell. Biol. *15*, 3654–3663.

Livneh, E., Glazer, L., Segal, D., Schlessinger, J., and Shilo, B.Z. (1985). The *Drosophila* EGF receptor gene homolog: conservation of both hormone binding and kinase domains. Cell *40*, 599–607.

Lu, X., Chou, T.B., Williams, N.G., Roberts, T., and Perrimon, N. (1993). Control of cell fate determination by $p21^{ras}$/Ras1, an essential component of *torso* signaling in *Drosophila*. Genes Dev. *7*, 621–632.

Madhavan, M., and Schneiderman, H.A. (1977). Histological analysis of the dynamics of growth of imaginal discs and histoblast nests during the larval development of *Drosophila melanogaster*. Wilhelm Roux's Arch. *183*, 269–305.

Milan, M., Campuzano, S., and Garcia-Bellido, A. (1996). Cell cycling and patterned cell proliferation in the wing primordium of *Drosophila*. Proc. Natl. Acad. Sci. USA *93*, 640–645.

Mittnacht, S., Paterson, H., Olson, M.F., and Marshall, C.J. (1997). Ras signaling is required for inactivation of the tumour suppressor pRb cell-cycle control protein. Curr. Biol. *7*, 219–221.

Montagne, J., Stewart, M.J., Stocker, H., Hafen, E., Kozma, S.C., and Thomas, G. (1999). *Drosophila* S6 kinase: a regulator of cell size. Science *285*, 2126–2129.

Morata, G., and Ripoll, P. (1975). Minutes: mutants of *Drosophila* autonomously affecting cell division rate. Dev. Biol. *42*, 211–221.

Mulcahy, L.S., Smith, M.R., and Stacey, D.W. (1985). Requirement for *ras* proto-oncogene function during serum-stimulated growth of NIH 3T3 cells. Nature *313*, 241–243.

Neufeld, T.P., de la Cruz, A.D.A., Johnston, L.A., and Edgar, B.A. (1998). Coordination of growth and cell division in the *Drosophila* wing. Cell *93*, 1183–1193.

Neuman-Silberberg, F.S., Schejter, E., Hoffman, F.M., and Shilo, B.Z. (1984). The *Drosophila ras* oncogenes: structure and nucleotide sequence. Cell *37*, 1027–1033.

Nishida, Y., Hata, M., Ayaki, T., Ryo, H., Yamagata, M., Shimizu, K., and Nishizuka, Y. (1988). Proliferation of both somatic and germ cells is affected in the *Drosophila* mutants of *raf* proto-oncogene. EMBO J. *7*, 775–781.

Peeper, D.S., Upton, T.M., Ladha, M.H., Neuman, E., Zalvide, J., Bernards, R., DeCaprio, J.A., and Ewen, M.E. (1997). Ras signaling linked to the cell-cycle machinery by the retinoblastoma protein. Nature *386*, 177–181.

Pignoni, F., and Zipursky, S. (1997). Induction of *Drosophila* eye development by decapentaplegic. Development *124*, 271–278.

Polymenis, M., and Schmidt, E.V. (1997). Coupling of cell division to cell growth by translational control of the G1 cyclin CLN3 in yeast. Genes Dev. *11*, 2522–2531.

Richardson, H.E., O'Keefe, L.V., Reed, S.I., and Saint, R. (1993). A *Drosophila* G1-specific *cyclin E* homolog exhibits different modes of expression during embryogenesis. Development *119*, 673–690.

Rommel, C., and Hafen, E. (1998). Ras—a versatile cellular switch. Curr. Opin. Genet. Dev. *8*, 412–418.

Schnepp, B., Grumbling, G., Donaldson, T., and Simcox, A. (1996). Vein is a novel component in the *Drosophila* epidermal growth factor receptor pathway with similarity to the neuregulins. Genes Dev. *10*, 2302–2313.

Schnorr, J.D., and Berg, C.E. (1996). Differential activity of *ras1* during patterning of the *Drosophila* dorsoventral axis. Genetics *144*, 1545–1557.

Sears, R., Leone, G., DeGregori, J., and Nevins, J.R. (1999). Ras enhances Myc protein stability. Mol. Cell *3*, 169–179.

Simcox, A. (1997). Differential requirement for EGF-like ligands in *Drosophila* wing development. Mech. Dev. *62*, 41–50.

Simcox, A.A., Grumbling, G., Schnepp, B., Bennington-Mathias, C., Hersperger, E., and Shearn, A. (1996). Molecular, phenotypic, and expression analysis of vein, a gene required for growth of the *Drosophila* wing disc. Dev. Biol. *177*, 475–489.

Sinn, E., Muller, W., Pattengale, P., Tepler, I., Wallace, R., and Leder, P. (1987). Coexpression of MMTV/v-Ha-*ras* and MMTV/*c-myc* genes in transgenic mice: synergistic action of oncogenes in vivo. Cell *49*, 465–475.

Struhl, G., and Basler, K. (1993). Organizing activity of wingless protein in *Drosophila*. Cell *72*, 527–540.

Sturtevant, M.A., and Bier, E. (1995). Analysis of the genetic hierarchy guiding wing vein development in *Drosophila*. Development *121*, 785–801.

Sturtevant, M.A., Roark, M., and Bier, E. (1993). The *Drosophila rhomboid* gene mediates the localized formation of wing veins and interacts genetically with components of the EGF-R signaling pathway. Genes Dev. *7*, 961–973.

Thevelein, J.M., and de Winde, J.H. (1999). Novel sensing mechanisms and targets for the cAMP-protein kinase A pathway in the yeast *Saccharomyces cerevisiae*. Mol. Microbiol. *33*, 904–918.

Verdu, J., Buratovich, M.A., Wilder, E.L., and Birnbaum, M.J. (1999). Cell-autonomous regulation of cell and organ growth in Drosophila by Akt/PKB. Nat. Cell Biol. *1*, 500–506.

Warner, J.R. (1999). The economics of ribosome biosynthesis in yeast. Trends Biochem. Sci. *24*, 437–440.

Weigmann, K., Cohen, S.M., and Lehner, C.F. (1997). Cell cycle progression, growth and patterning in imaginal discs despite inhibition of cell division after inactivation of *Drosophila* Cdc2 kinase. Development *124*, 3555–3563.

Weinkove, D., Neufeld, T.P., Twardzik, T., Waterfield, M.D., and Leevers, S.J. (1999). Regulation of imaginal disc cell size, cell number and organ size by *Drosophila* class I(A) phosphoinositide 3-kinase and its adaptor. Curr. Biol. *9*, 1019–1029.

Winston, J.T., Coats, S.R., Wang, Y.Z., and Pledger, W.J. (1996). Regulation of the cell cycle machinery by oncogenic *ras*. Oncogene *12*, 127–134.

Xu, T., and Rubin, G.M. (1993). Analysis of genetic mosaics in developing and adult *Drosophila* tissues. Development *117*, 1223–1237.